Full-Boltzmann-equation solutions of the acoustic-phonon-limited conductivity and Hall mobilities for *p*-type silicon and germanium

Frank Szmulowicz and Frank L. Madarasz
University of Dayton Research Institute, 300 College Park Avenue, Dayton, Ohio 45469
(Received 25 October 1982; revised manuscript received 20 December 1982)

Acoustic-phonon-limited conductivity and Hall mobilities for *p*-type silicon and germanium have been calculated from solutions of the full Boltzmann equation without the relaxation-time approximation. Using the deformation-potential scattering theory of Tiersten, we obtain the necessary hole—acoustic-phonon transition rates, with no adjustable parameters, as a first-principles input into the transport equations. Excellent agreement is found for both mobilities in silicon, and the conductivity mobility in germanium, as compared with experimental data. The Hall mobility for germanium is within 12% of the measured Hall mobility—the closest agreement to date for a first-principles theory. The success of this calculation is due to the inclusion of all three top valence bands, careful treatment of the scattering matrix elements, and the use of the full-Boltzmann-equation solutions to obtain the transport coefficients. Results of our calculation confirm the quantitative accuracy of the deformation-potential theory.

I. INTRODUCTION

Acoustic-phonon-limited electronic transport in diamond[1–23] and in zinc-blende-type[24–26] structures has often been modeled within the framework of the deformation-potential theory. Within the theory the strength of the carrier-phonon interaction is governed by an experimentally determined set of deformation-potential parameters. These parameters are obtained from experiments which measure shifts and distortions of the bands upon application of selected strains to the crystal.[27–37] However, in some versions of the scattering theory it has been found necessary to regard these interaction parameters as adjustable in order to obtain a quantitative agreement with the transport data. This is particularly the case in the transport calculations for *p*-type materials[8–12,15,19–22] where either effective deformation potentials or the relaxation times were fitted to the transport data.

The need for adjustment of parameters arises as a result of approximations introduced in the theoretical treatment of the full deformation-potential scattering theory. It is a common simplification to use a relaxation-time approximation for the solution of the Boltzmann equation. One of the most elaborate examples of such a model is provided in the work of Bir, Normantas, and Picus.[4] This model employs separate intraband and interband relaxation rates which depend on averaged deformation-potential constants whose magnitudes are varied in the calculation. Other authors have considered separate relaxation times for each band, with a common effective deformation potential, but without any interband coupling.[8,12,14,20,23]

Along with the relaxation-time approximation, the degree to which the full nonspherical nonparabolic nature of the valence bands has been taken into account, at various points in the calculation, has varied from one theoretical treatment to another. The simplest approach, as for example that taken by Bir *et al.*[4] and by Costato *et al.*,[12] is to consider just the two top valence bands—the heavy-hole band and the light-hole band. Both bands are treated as spherical parabolic. A slightly more complex model treats the light-hole band on the average as nonparabolic. This model was set by Ottaviani *et al.*[14] who also considered a single nonspherical but parabolic band model along with a Monte Carlo technique in order to study the effects of anisotropy.[14] Asche and von Borzeszkowski,[20] on the other hand, studied the effect of band nonparabolicity on mobilities. In order to account for band nonparabolicities as accurately as possible they calculated the hole density-of-states factors in the relaxation rates by using a spherically averaged Kane[38] secular equation, which results in isotropic bands. Following Asche and von Borzeszkowski, Nakagawa and Zukotynski[8] performed a calculation in the same spirit but did not spherically average the bands. And, more recently, Takeda, Sakui, and Sakata[23] repeated the work of Nakagawa and Zukotynski, but in addition they

considered the spin-orbit split-off band's contribution to the mobility.[23] In view of the number of approximations introduced in previous treatments of the problem it appears worthwhile to approach the problem again from a first-principles point of view, without the band shape or the relaxation-time approximations.

Except for the treatments of Tiersten[1] and Lawaetz[2] for Ge, a complete implementation of the deformation-potential theory has not been pursued from first principles. These two authors did not use the relaxation-time approximation, but instead each solved the Boltzmann equation directly. Tiersten used the deformation-potential theory of Whitfield[39] and the vector mean-free-path theory of Price[40] to solve the Boltzmann equation. Lawaetz, on the other hand, used the transition rates of Bir and Pikus[3] and solved the Boltzmann equation by expanding the distribution function in cubic harmonics. Both methods were found to agree with one another to within 2% for the conductivity mobility of Ge and were within a few percent of the experimental mobility. In addition, Lawaetz calculated the Hall mobility and other galvanomagnetic coefficients. Here he found that his results could not be reconciled with the independently measured set of deformation-potential parameters. Partly, this discrepancy can be attributed to the incomplete knowledge of the parameters, or to the quality of data used for comparison with the theory. In our work, however, we will show that the results for the Hall mobility, at least, can be improved by treating the light-hole band as nonparabolic, which was done by neither Tiersten nor Lawaetz.

No comparable treatment to that of Tiersten or Lawaetz has been tried for p-type silicon. Whereas germanium has a large 0.30-eV spin-orbit splitting, in silicon the corresponding splitting is only 0.044 eV. Therefore, its bands are decidedly more nonparabolic than is the case for germanium. Even in the case of germanium we will show that light holes dominate the Hall mobility, and the light-hole band's nonparabolicity, however small, does influence the results. To this end we have calculated hole–acoustic-phonon transition rates for Si and Ge using experimentally determined deformation-potential parameters. As we have pointed out in our previous papers,[41,42] the inclusion of the full nonparabolic nature of the Si valence-band system results in a strikingly energy-dependent set of transition probabilities. Parabolic bands, though, lead to energy-independent transition probabilities.

The goal of the present work is to fully implement the deformation-potential theory for the calculation of conductivity and Hall mobilities in Si and Ge, with emphasis on Si, in the acoustic-phonon-limited regime. By using the eigenfunctions obtained from the numerical solution of the full 6×6 $\vec{k}\cdot\vec{p}$ Hamiltonian we make no approximations concerning the nonspherical nonparabolic nature of the Si valence-band structure. Our transition probabilities are energy dependent and depend on both the incident and scattered hole wave vectors as well. We solve the Boltzmann equation directly, by a variant of the method used by Lawaetz,[2] for the distribution function. Then, analogously to Lawaetz, we obtain the conductivity and Hall mobilities.

In Sec. II we formulate the transport theory to be used in the present work. Our formalism differs in a few details from that of Lawaetz who, in addition, has not provided the full derivation. We include in Sec. III details of the computational procedure. Section IV is used as a test of the computational scheme. Here we use the parameters of Tiersten and Lawaetz for Ge and exhibit an overall agreement between our respective results. In the case of the Hall mobility we show an overall improvement in our results as compared with experiment. Section V is devoted to the presentation of results for Si. Conclusions are presented last.

II. THEORY

Our task is to solve the Boltzmann equation for the hole distribution functions for p-type Si when both the electric field $\vec{F}$ and magnetic field $\vec{B}$ are present. With the distribution functions we are to calculate both the conductivity mobility μ_c and the Hall mobility μ_H, and their ratio $\mu_H/\mu_c=r$ (the so-called Hall r factor).

The Boltzmann equation is[2]

$$\left[\frac{e}{\hbar}\vec{F}\cdot\vec{\nabla}_{\vec{k}}-\frac{e}{\hbar^2}\vec{B}\cdot[\vec{\nabla}_{\vec{k}}E_N(\vec{k})\times\vec{\nabla}_{\vec{k}}]\right]f_N(\vec{k}) =S_{\rm op}f_N(\vec{k}) , \quad (2.1)$$

where $f_N(\vec{k})$ is the steady-state distribution function for valence band N of energy $E_N(\vec{k})$ at wave vector $\vec{k}$ in the Brillouin zone of Si. $S_{\rm op}$ is the scattering operator given by

$$S_{\rm op}f_N(\vec{k})=\frac{V}{(2\pi)^3}\sum_{M=1}^{3}\int d\vec{k}'[f_M(\vec{k}')-f_N(\vec{k})] \times W_{NM}(\vec{k},\vec{k}') , \quad (2.2)$$

V is the volume of the crystal, and the sum over M is carried over the three top valence bands of Si. The transition probabilities for hole scattering by acoustic phonons between bands N at $\vec{k}$ and M at $\vec{k}'$ were expressed in our previous paper as[42]

$$W_{NM}(\vec{k},\vec{k}')=\frac{\pi k_B T}{2V\hbar}\left[\sum_i \sum_{L,L'} A^i_{NL,ML'}(E_N(\vec{k}))\left[\sum_{\mu=1}^{l_i} K_L^{i\mu}(\hat{k})K_{L'}^{i\mu}(\hat{k}')\right]\right]\delta(E_N(\vec{k})-E_M(\vec{k}')) . \tag{2.3}$$

Here k_B is the Boltzmann constant, T is the absolute temperature, and $K_L^{i\mu}(\hat{k})$ is a normalized cubic harmonic in direction $\hat{k}$ with angular index L transforming like the μth row of the ith irreducible representation of O_h with dimension l_i. The coefficients A were fitted to the transition rates in our previous paper on angular variations of the rates.[42] These rates were calculated by us in Ref. 41 using the deformation-potential theory of Tiersten.[1] In that paper we used the three top valence bands of silicon taking into account both their nonparabolicity and anisotropy. Similar rate calculations were performed by Tiersten and Lawaetz in the parabolic band regime for Ge.[1,2] In the rather good elastic scattering approximation of holes by acoustic phonons, the expansion coefficients A are only functions of one of the holes' energies.[42] The δ function in (2.3) reflects this energy-conservation condition.

The Boltzmann equation (2.1) can be written more concisely as[2]

$$(\vec{F}\cdot\vec{F}_{op}+\vec{B}\cdot\vec{B}_{op})f_N(\vec{k})=S_{op}f_N(\vec{k}) , \tag{2.4}$$

where from (2.1)

$$\vec{F}_{op}=\frac{e}{\hbar}\vec{\nabla}_{\vec{k}} , \tag{2.5}$$

$$\vec{B}_{op}=-\frac{e}{\hbar^2}\vec{\nabla}_{\vec{k}}E_N(\vec{k})\times\vec{\nabla}_{\vec{k}} . \tag{2.6}$$

To first order in both the electric and magnetic fields, the steady-state distribution function can be written as[2]

$$f_N(\vec{k})=f_N^0(\vec{k})+F\psi_{10}^N(\vec{k})+FB\psi_{11}^N(\vec{k}) , \tag{2.7}$$

where ψ_{10}^N reflects the deviation of the distribution function from its thermal-equilibrium value

$$f_N^0(\vec{k})=\exp\{-[E_N(\vec{k})-\mu]/k_BT\}$$
$$=f_N^0(E_N(\vec{k})) , \tag{2.8}$$

where μ is the chemical potential upon application of the electric field. ψ_{11}^N, similarly, is the added deviation from $f_N^0(\vec{k})$ when, additionally, a low magnetic field $\vec{B}$ is turned on. Inserting Eq. (2.7) for $f_N(\vec{k})$ into Eq. (2.4), and equating the same powers of $\vec{F}$ and $\vec{B}$ on both sides of (2.4), one obtains

$$(\hat{F}\cdot\vec{F}_{op})f_N^0(\vec{k})=S_{op}\psi_{10}^N(\vec{k}) \tag{2.9a}$$

and

$$(\hat{B}\cdot\vec{B}_{op})\psi_{10}^N(\vec{k})=S_{op}\psi_{11}^N(\vec{k}) , \tag{2.9b}$$

where $\hat{F}$ and $\hat{B}$ are unit vectors in the directions of $\vec{F}$ and $\vec{B}$, respectively. Equations (2.9a) and (2.9b) reflect the ascending hierarchy of equations needed to evaluate high-order F^nB^m perturbations of the distribution function. Equations for general order n,m in the series have been exhibited by Lawaetz.[2] For calculations of conductivity and Hall mobilities we need go no further than the first two equations (2.9a) and (2.9b). This is consistent with typically low magnitudes of the electric and magnetic fields used in the Hall experiments. Incidentally, the hot-electron effects, in the non-Ohmic regime, necessitate higher-order F powers in the $f_N(\vec{k})$ expansion [Eq. (2.7)].

We solve the Boltzmann equation using the method developed by Lawaetz. For this we expand ψ_{10}^N and ψ_{11}^N in a cubic harmonic series

$$\psi_{10}^N(\vec{k})=f_N^0(\vec{k})\sum_{k,\eta,\lambda'}\phi_{N\lambda'}^{k\eta}(E_N(\vec{k}))K_{\lambda'}^{k\eta}(\hat{k}) , \tag{2.10a}$$

$$\psi_{11}^N(\vec{k})=f_N^0(\vec{k})\sum_{k,\eta,\lambda'}\chi_{N\lambda'}^{k\eta}(E_N(\vec{k}))K_{\lambda'}^{k\eta}(\hat{k}) , \tag{2.10b}$$

with expansion coefficients ϕ and χ, respectively. Note that the most rapid energy variations of ψ_{10}^N and ψ_{11}^N have been factored out in

$$f_N^0(\vec{k})=f_N^0(E_N(\vec{k})) , \tag{2.11}$$

leaving relatively smooth functions ϕ and χ.

A. Solution of the Boltzmann equation

Our method for solving Eqs. (2.9) is sufficiently different from that of Lawaetz to merit its own development in this subsection. Whereas Lawaetz[2] multiplies both sides of Eqs. (2.9) on the left by a cubic harmonic $K_{\lambda''}^{j\nu}(\hat{k})$ and integrates over the angle $\hat{k}$, we, in addition, multiply these equations by $\delta(E_N(\vec{k})-\mathscr{E})$ and integrate over the whole Brillouin zone. The field term in Eq. (2.9a) becomes then

$$\frac{e}{\hbar}\hat{F}\cdot\int d\vec{k}\,K_{\lambda''}^{j\nu}(\hat{k})\delta(E_N(\vec{k})-\mathscr{E})\vec{\nabla}_{\vec{k}}f_N^0(\vec{k}) . \tag{2.12}$$

In order to carry out the Brillouin-zone integral in Eq. (2.12), we define for each band, $N=S$, L, and H (spin-orbit, light, and heavy valence bands, respectively), functions γ_N, where

$$k_N^2 \equiv \frac{2m_0}{\hbar^2}\gamma_N(E_N(\vec{k}),\hat{k}) , \tag{2.13}$$

and m_0 is the free-electron mass. Most conveniently,

$$\frac{\hbar^2}{2m_0}=1 , \tag{2.14}$$

in units of Ry a.u.^{2}, where Ry$=1$ rydberg$=13.6058$ eV, and 1 a.u. is the atomic unit of length equal to 1 Bohr radius which is equal to 0.5292×10^{-8} cm. As we will show, the atomic units are a more natural set of units to carry out the calculation than the units we employed in the first two publications.[41,42]

Equation (2.13) suggests the change of the integration element to

$$k^2dk=\frac{1}{2}\left[\frac{2m_0}{\hbar^2}\right]^{3/2}\gamma_N^{1/2}(E_N(\vec{k}),\hat{k}) \times\frac{d\gamma_N(E_N(\vec{k}),\hat{k})}{dE_N(\vec{k})}dE_N(\vec{k}) . \tag{2.15}$$

Altogether, with Eqs. (2.8) and (2.15), Eq. (2.12) assumes the form

$$-\frac{ef_N^0(\mathscr{E})}{2\hbar k_B T}\hat{F}\cdot\vec{g}_{N\lambda''}^{j\nu}(\mathscr{E}) , \tag{2.16}$$

where

$$\vec{g}_{N\lambda''}^{j\nu}(\mathscr{E})=\left[\frac{2m_0}{\hbar^2}\right]^{3/2}\int d\hat{k}\,K_{\lambda''}^{j\nu}(\hat{k})\gamma_N^{1/2}(\mathscr{E},\hat{k}) \times\frac{d\gamma_N(\mathscr{E},\hat{k})}{d\mathscr{E}} \times[\vec{\nabla}_{\vec{k}}E_N(\vec{k})]_{\mathscr{E}} , \tag{2.17}$$

and the energy gradient is evaluated on the constant energy $\mathscr{E}$ surface. Since γ is in rydbergs, $\vec{g}$ is in a.u.$^{-2}$

The collision term, on the right-hand side of Eq. (2.9a), can be similarly simplified. But first we note that the expansion coefficients A in Eq. (2.3) for W_{NM} were given in Refs. 41 and 42 in units of eV^{2}cm^3/erg. This prefactor can also be written in atomic units as 7.9537×10^{11} Ry a.u.^{3} In the old units the A's were on the order of 10^{-11} so that in the new units the A's are on the order of unity. Multiplying Eq. (2.9a) by $K_{\lambda''}^{j\nu}(\hat{k})\delta(E_N(\vec{k})-\mathscr{E})$ and integrating over $\vec{k}$ and $\vec{k}'$, with ψ_{10}^N given by Eq. (2.10a), $S_{\rm op}$ defined by Eq. (2.2), and W_{NM} by Eq. (2.3), and the change of variables Eq. (2.15), we obtain, for the right-hand side (rhs),

$$\frac{1}{4}\frac{k_BT}{(4\pi)^2\hbar}f_N^0(\mathscr{E})\sum_{k,M,\eta,\lambda'}S_{N\nu\lambda'',M\eta\lambda'}^{jk}(\mathscr{E})\phi_{M\lambda'}^{k\eta}(\mathscr{E}) . \tag{2.18}$$

Here, we define the scattering matrix S as

$$S_{N\nu\lambda'',M\eta\lambda'}^{jk}(\mathscr{E})=\sum_{i,\mu,L,L'}\Big[\langle j\nu\lambda''\,|\,\Gamma_N\,|\,i\mu L\rangle A_{NL,ML'}^{i}\langle i\mu L'\,|\,\Gamma_M\,|\,k\eta\lambda'\rangle - \delta_{NM}\sum_{P=1}^{3}\langle j\nu\lambda'',k\eta\lambda'\,|\,\Gamma_N\,|\,i\mu L\rangle A_{NL,PL'}^{i}\langle i\mu L'\,|\,\Gamma_P\,|\,1\rangle\Big] . \tag{2.19}$$

The bras and kets denote angular Brillouin-zone integrals between normalized cubic harmonics

$$\langle\hat{k}\,|\,j\nu\lambda\rangle=K_\lambda^{j\nu}(\hat{k}) , \tag{2.20}$$

and the local operator Γ_N is defined as

$$\Gamma_N(\mathscr{E},\hat{k})=\langle\hat{k}\,|\,\Gamma_N(\mathscr{E})\,|\,\hat{k}\rangle=\left[\frac{2m_0}{\hbar^2}\right]^{3/2}\gamma_N^{1/2}(\mathscr{E},\hat{k})\frac{d\gamma_N(\mathscr{E},\hat{k})}{d\mathscr{E}} . \tag{2.21}$$

It is very important to the rest of the analysis that

$$\Gamma_N(\mathscr{E},R\hat{k})=\Gamma_N(\mathscr{E},\hat{k}) , \tag{2.22}$$

for all rotations $R\in O_h$, the cubic point group, so that $\Gamma_N(\mathscr{E},\hat{k})$ transforms like the identity representation. The property (2.22) follows trivially from the defining Eq. (2.21) for Γ_N and from (2.13) for γ_N, where one has

$$E_N(R\vec{k})=E_N(\vec{k}) \tag{2.23}$$

from the invariance of the electron Hamiltonian with respect to space-group operations of the crystal. It is easy to show that the collision matrix S, Eq. (2.19), has units of (Ry a.u.^{3})$^{-1}$. The advantage of the form Eq. (2.19) over the one used by Lawaetz is that our matrix S is symmetric in indices $(Nj\nu\lambda,Mk\eta\lambda')$.

Since Γ_N belongs to the identity representation we may employ orthogonality of the cubic harmonics with

respect to the representation and partner indices, i.e., in Eq. (2.19) $j=k$ and $\nu=\eta$, so that

$$S^{jk}_{N\nu\lambda'',M\eta\lambda'}(\mathscr{E})\equiv S^{j\nu}_{N\lambda'',M\lambda'}(\mathscr{E})\delta_{jk}\delta_{\nu\lambda}=\sum_{L,L'}\left[\langle j\nu\lambda''\,|\,\Gamma_N\,|\,j\nu L\rangle A^j_{NL,ML'}\langle j\nu L'\,|\,\Gamma_M\,|\,j\nu\lambda'\rangle - \delta_{NM}\sum_{P=1}^{3}\langle j\nu\lambda'',j\nu\lambda'\,|\,\Gamma_N\,|\,\alpha L\rangle A^{\alpha}_{NL,PL'}\langle\alpha L'\,|\,\Gamma_P\,|\,1\rangle\right]. \tag{2.24}$$

We use α in Eq. (2.24) to denote the one-dimensional identity representation.

Combining results of Eqs. (2.16), (2.18), and (2.24) the following system of linear equations results:

$$-2e\left[\frac{4\pi}{k_BT}\right]^2\hat{F}\cdot\vec{g}^{\,j\nu}_{N\lambda''}=\sum_{M,\lambda'}S^{j\nu}_{N\lambda'',M\lambda'}\phi^{j\nu}_{M\lambda'}\,. \tag{2.25}$$

Equation (2.25) is to be solved for the expansion coefficients ϕ. As can be seen, the system of linear equations factors out into separate problems for different irreducible representation j and partner indices ν. If we go one step further, we can show that solutions ϕ have a simple dependence on the partner index ν. From the matrix-element theorems we can write the integrals in Eq. (2.24) as follows[43]:

$$\langle j\nu\lambda''\,|\,\Gamma_N\,|\,j\nu\lambda\rangle=\frac{1}{l_j}\sum_{\mu=1}^{l_j}\langle j\mu\lambda''\,|\,\Gamma_N\,|\,j\mu\lambda\rangle\,, \tag{2.26a}$$

for all $1\le\nu\le l_j$, where l_j is the dimensionality of the jth irreducible representation of O_h, since Γ_N transforms like the identity representation. Similarly, the "Gaunt-type" integral of three cubic harmonics in Eq. (2.24),

$$\langle j\nu\lambda'',j\nu\lambda'\,|\,\Gamma_N\,|\,\alpha L\rangle=\frac{1}{l_j}\sum_{\mu=1}^{l_j}\langle j\mu\lambda'',j\mu\lambda'\,|\,\Gamma_N\,|\,\alpha L\rangle\,, \tag{2.26b}$$

where $\Gamma_N\,|\,\alpha L\rangle$ transforms like the identity representation since $\langle\hat{k}\,|\,\alpha L\rangle$ is a cubic harmonic for the identity representation. Equations (2.26a) and (2.26b) show then that the index ν on S in Eqs. (2.24) and (2.25) is redundant.

Examining the $\vec{g}$ vector, Eq. (2.17), shows that j must belong to the vector representation Γ_{15}, since $\vec{\nabla}_{\vec{k}}E_N(\vec{k})$ transforms like Γ_{15} [or δ in the notation of Von der Lage and Bethe[44] (VdLB)]. For all other j the left-hand side (lhs) of Eq. (2.25) is zero so that $\phi=0$ for $j\neq\delta$. Rows of the δ representation ν can be labeled by the Cartesian coordinates x, y, and z. The matrix-element theorem expressed by Eq. (2.26) can be used for g as well, with the result that for fixed ν

$$\vec{g}^{\,j\nu}_{N\lambda''}(\mathscr{E})=\left[\frac{1}{l_j}\sum_{\mu=1}^{l_j}\int d\hat{k}\,K^{j\mu}_{\lambda''}(\hat{k})\Gamma_N(\mathscr{E},\hat{k})\times\left[\frac{\partial E_N(\vec{k})}{\partial k_\mu}\right]_{\mathscr{E}}\right]\hat{e}_\nu \equiv\{-[G^j_{N\lambda''}(\mathscr{E})/2]\}\hat{e}_\nu\,, \tag{2.27}$$

where $\hat{e}_\nu$ is a unit vector in the νth direction. With the use of the above developments, Eq. (2.25) becomes

$$e\left[\frac{4\pi}{k_BT}\right]^2\hat{F}\cdot\hat{e}_\nu G^j_{N\lambda''}(\mathscr{E})=\sum_{M\lambda'}S^j_{N\lambda'',M\lambda'}(\mathscr{E})\phi^{j\nu}_{M\lambda'}(\mathscr{E})\,, \tag{2.28}$$

which has the solution

$$\phi^{j\nu}_{N\lambda'}=e\left[\frac{4\pi}{k_BT}\right]^2\hat{F}\cdot\hat{e}_\nu\times\left[\sum_{M\lambda''}[S^j_{N\lambda',M\lambda''}(\mathscr{E})]^{-1}G^j_{M\lambda''}(\mathscr{E})\right] \equiv e\left[\frac{4\pi}{k_BT}\right]^2\hat{F}\cdot\hat{e}_\nu[\theta^j_{N\lambda'}(\mathscr{E})]\,, \tag{2.29}$$

where the directional dependence is contained in $\hat{F}\cdot\hat{e}_\nu$. If we define

$$\vec{\Phi}_N(\mathscr{E},\hat{k})\equiv\sum_\lambda e\left[\frac{4\pi}{k_BT}\right]^2\begin{bmatrix}K^{\delta x}_\lambda(\hat{k})\hat{e}_x\\K^{\delta y}_\lambda(\hat{k})\hat{e}_y\\K^{\delta z}_\lambda(\hat{k})\hat{e}_z\end{bmatrix}\theta^\delta_{N\lambda}(\mathscr{E})\,, \tag{2.30}$$

then to first order in the electric field Eq. (2.7) can be written in the familiar form

$$f_N(\vec{k})=f^0_N(\vec{k})[1+\vec{F}\cdot\vec{\Phi}_N(\mathscr{E},\hat{k})]\,. \tag{2.31}$$

Clearly, the units of $\vec{\Phi}$ and ϕ are those of the (electric field)$^{-1}$, while those of θ are Ry a.u.

Equation (2.29) provides the solution for that part

of the distribution function which is perturbed by the application of the electric field only. The second part of the problem is the solution of Eq. (2.9b) for the part of the distribution function which is perturbed by the simultaneous application of the magnetic field. As for the rhs, we use the expansion (2.10b) for ψ_{11}, multiply the rhs by

$$K^{j\nu}_{\lambda''}(\hat{k})\delta(E_N(\vec{k})-\mathscr{E}) ,$$

and integrate over $\vec{k}$. This part of the calculation is identical to the calculation above with χ replacing ϕ, so that the right-hand side becomes

$$\frac{1}{4}\frac{k_B T}{(4\pi)^2\hbar}f^0_N(\mathscr{E})\sum_{M\lambda'} S^{j}_{N\lambda'',M\lambda'}(\mathscr{E})\chi^{j\nu}_{M\lambda'}(\mathscr{E}) , \tag{2.32}$$

where χ are the expansion coefficients for ψ^N_{11} in Eq. (2.10b). On the lhs, Eq. (2.9b), ψ^N_{10} is the solution obtained earlier in Eq. (2.30), and the $\vec{B}_{op}$ is given by Eq. (2.6). $\vec{B}_{op}$, due to the presence of the cross vector product, commutes with any function of energy, such as $f^0_N(E_N(\vec{k}))$, matrices S and G, and expansion coefficients ϕ. Multiplying the field term, Eq. (2.9b), by

$$K^{j\nu}_{\lambda''}(\hat{k})\delta(E_N(\vec{k})-\mathscr{E}) ,$$

and integrating over $\vec{k}$, we obtain, for the left-hand side,

$$-\frac{e}{2\hbar^2}f^0_N(\mathscr{E})\sum_{\mu\lambda'''}\phi^{i\mu}_{N\lambda'''}(\mathscr{E})\hat{B}\cdot\vec{H}^{i\mu,j\nu}_{N\lambda''',N\lambda''}(\mathscr{E}) , \tag{2.33}$$

where the magnetic field matrix is given by

$$\vec{H}^{i\mu,j\nu}_{N\lambda''',N\lambda''}(\mathscr{E})=\int d\hat{k}\,K^{j\nu}_{\lambda''}(\hat{k})\Gamma_N(\mathscr{E},\hat{k}) \times[\vec{\nabla}_{\vec{k}}E_N(\vec{k})\times\vec{\nabla}_{\vec{k}}]_{\mathscr{E}}K^{i\mu}_{\lambda'''}(\hat{k}) , \tag{2.34}$$

evaluated on the constant energy $\mathscr{E}$ surface. The sum over $\mu\lambda'''$ in Eq. (2.33) comes about because of the cubic harmonic expansion of ψ^N_{10}. Clearly, index $i=\delta$ and $\mu=x$, y, or z. H is in (a.u.)$^{-1}$.

As we shall show later, Eq. (2.52b), for the Hall mobility calculation we need only the part of ψ^N_{11} which transforms like the vector representation $\Gamma_{15}=\delta$, so that $j=\delta$ as well. We shall not calculate the part of ψ^N_{11} transforming like the $\Gamma_{25}=\epsilon'$ representation since it is irrelevant for our goals. We note that

$$[\vec{\nabla}_{\vec{k}}E_N(\vec{k})\times\vec{\nabla}_{\vec{k}}]_{\mathscr{E}}\equiv\vec{h}_N(\mathscr{E},\hat{k}) \tag{2.35}$$

transforms like a pseudovector according to the $\Gamma'_{15}=\delta'$ representation. The magnetic field matrix, Eq. (2.34), can be shown to be nonvanishing for the choice $i=j=\delta$ since the direct product

$$\Gamma_{15}\otimes\Gamma'_{15}=\Gamma_{15}+\Gamma_{25}+\Gamma'_1+\Gamma'_{12} \tag{2.36}$$

contains Γ_{15} in its decomposition. The pseudovector operator h transforms under coordinate rotations according to

$$P(R)h_pP(R^{-1})=\sum_{q=1}^{3}\Gamma^m_{qp}(R)h_q , \tag{2.37}$$

where $P(R)$ are the scalar rotation operators which operate on functions, as opposed to rotation matrices R which operate on vectors. $\Gamma^m(R)$ is the matrix for the pseudovector Γ'_{15} irreducible representation of O_h.

With these preliminaries, we can show that

$$\begin{aligned}\vec{H}^{\delta\mu,\delta\nu}_{N\lambda''',N\lambda''}(\mathscr{E})&=\langle\delta\nu\lambda''\,|\,\Gamma_N\vec{h}(\mathscr{E})\,|\,\delta\mu\lambda'''\rangle\\&=\tfrac{1}{48}\sum_{R\in O_h}\sum_p\hat{e}_p\langle P(R)\delta\nu\lambda''\,|\,\Gamma_N(\mathscr{E})P(R)h_p(\mathscr{E})P(R^{-1})\,|\,P(R)\delta\mu'\lambda'''\rangle\\&=\tfrac{1}{48}\sum_{R\in O_h}\sum_{p,q,\nu',\mu'}\hat{e}_p\Gamma^{\delta}_{\nu'\nu}(R)\Gamma^m_{qp}(R)\Gamma^{\delta}_{\mu'\mu}(R)\langle\delta\nu'\lambda''\,|\,\Gamma_N(\mathscr{E})h_q(\mathscr{E})\,|\,\delta\mu'\lambda'''\rangle .\end{aligned} \tag{2.38}$$

Summing over the 48 point-group rotations of O_h, we obtain the following result:

$$\vec{H}^{\delta\mu,\delta\nu}_{N\lambda''',N\lambda''}(\mathscr{E})=\tfrac{1}{6}\sum_p\hat{e}_p\epsilon_{\nu p\mu}\left[\sum_{\nu',p',\mu'}\epsilon_{\nu'p'\mu'}\langle\delta\nu'\lambda''\,|\,\Gamma_N(\mathscr{E})h_{p'}(\mathscr{E})\,|\,\delta\mu'\lambda'''\rangle\right]\equiv\tfrac{1}{6}\sum_p\hat{e}_p\epsilon_{\nu p\mu}\mathscr{H}^{\delta}_{N\lambda''',N\lambda''}(\mathscr{E}) , \tag{2.39}$$

where $\epsilon_{\nu p\mu}$ is the Levi-Cività symbol.

Therefore, expression (2.33) becomes

$$-\frac{e}{12\hbar^2}f_N^0(\mathscr{E})\sum_{\mu,\lambda'''}\phi_{N\lambda'''}^{\delta\mu}(\mathscr{E})\sum_p(\hat{e}_p\cdot\hat{B})\epsilon_{\nu p\mu}\mathscr{H}_{N\lambda''',N\lambda''}^{\delta}(\mathscr{E}) , \tag{2.40}$$

and substituting Eq. (2.29) for ϕ gives

$$-\left[\frac{4\pi e}{\hbar k_B T}\right]^2\frac{f_N^0(\mathscr{E})}{12}\sum_{\mu,\lambda'''}\theta_{N\lambda'''}^{\delta}(\mathscr{E})\hat{F}\cdot\hat{e}_\mu\sum_p(\hat{e}_p\cdot\hat{B})\epsilon_{\nu p\mu}\mathscr{H}_{N\lambda''',N\lambda''}^{\delta}(\mathscr{E}) . \tag{2.41}$$

Summing over μ and p, we finally obtain

$$+\left[\frac{4\pi e}{\hbar k_B T}\right]^2\frac{f_N^0(\mathscr{E})}{12}\sum_{\lambda'''}\theta_{N\lambda'''}^{\delta}(\mathscr{E})\mathscr{H}_{N\lambda''',N\lambda''}^{\delta}(\mathscr{E})(\hat{F}\times\hat{B})\cdot\hat{e}_\nu . \tag{2.42}$$

In combination with expression (2.32), the linear system of equations has the solution

$$\chi_{P\lambda}^{\delta\nu}=\left[\left[\frac{4\pi}{k_B T}\right]^3\frac{4\pi e^2}{\hbar}\right]\left[\frac{1}{3}\sum_{N,\lambda'',\lambda'''}(S_{P\lambda,N\lambda''}^{\delta})^{-1}\theta_{N\lambda'''}^{\delta}(\mathscr{E})\mathscr{H}_{N\lambda''',N\lambda''}^{\delta}(\mathscr{E})\right]$$
$$\times(\hat{F}\times\hat{B})\cdot\hat{e}_\nu\equiv\left[\frac{4\pi}{k_B T}\right]^3\frac{4\pi e^2}{\hbar}(\hat{F}\times\hat{B})\cdot\hat{e}_\nu\xi_{p\lambda}^{\delta}(\mathscr{E}) . \tag{2.43}$$

Defining

$$\vec{\mathrm{X}}_N(\mathscr{E},\hat{k})\equiv\sum_\lambda\left[\left[\frac{4\pi}{k_B T}\right]^3\frac{4\pi e^2}{\hbar}\right]\xi_{N\lambda}^{\delta}(\mathscr{E})$$
$$\times\begin{bmatrix}K_\lambda^{\delta x}(\hat{k})\hat{e}_x\\K_\lambda^{\delta y}(\hat{k})\hat{e}_y\\K_\lambda^{\delta z}(\hat{k})\hat{e}_z\end{bmatrix} , \tag{2.44}$$

the distribution function to first order in the magnetic field becomes

$$f_N(\vec{\mathrm{k}})=f_N^0(\vec{\mathrm{k}})[1+\vec{\mathrm{F}}\cdot\vec{\Phi}_N(\mathscr{E},\hat{k})$$
$$+(\vec{\mathrm{F}}\times\vec{\mathrm{B}})\cdot\vec{\mathrm{X}}_N(\mathscr{E},\hat{k})] . \tag{2.45}$$

B. Transport coefficients

The average thermal velocity in a material is given by

$$\langle\vec{\mathrm{V}}\rangle=\frac{\sum_{\vec{\mathrm{k}}}\sum_N\vec{\mathrm{V}}_N(\vec{\mathrm{k}})f_N(\vec{\mathrm{k}})}{\sum_{\vec{\mathrm{k}}}\sum_N f_N(\vec{\mathrm{k}})} , \tag{2.46}$$

where

$$\vec{\mathrm{V}}_N(\vec{\mathrm{k}})=\frac{1}{\hbar}\vec{\nabla}_{\vec{\mathrm{k}}}E_N(\vec{\mathrm{k}}) .$$

For a cubic material the relationship between the current density $\vec{\mathrm{J}}$ and the fields is[45]

$$\vec{\mathrm{J}}=pe\langle\vec{\mathrm{V}}\rangle=\sigma_0\vec{\mathrm{F}}+\sigma_0\mu_H(\vec{\mathrm{F}}\times\vec{\mathrm{B}})+\cdots , \tag{2.47}$$

where p is the carrier density, σ_0 is the conductivity

$$\sigma_0=pe\mu_c , \tag{2.48}$$

μ_c is the conductivity mobility, and μ_H is the Hall mobility. Hall experiments measure μ_H, although the data analysis for carrier densities requires μ_c. These are related by the so-called r factor

$$r=\mu_H/\mu_c . \tag{2.49}$$

We shall develop the necessary theoretical framework for evaluating μ_H and μ_c.

Since the distribution function contains terms proportional to F and FB, we can write Eq. (2.46) in the following form:

$$\langle\vec{\mathrm{V}}\rangle=\langle\vec{\mathrm{V}}_{10}\rangle F+\langle\vec{\mathrm{V}}_{11}\rangle FB , \tag{2.50}$$

which through Eqs. (2.47) and (2.48) provides us with the means of calculating mobilities. These equations are

$$\mu_c=\hat{F}\cdot\langle\vec{\mathrm{V}}_{10}\rangle , \tag{2.51a}$$

$$r\mu_c^2=(\hat{F}\times\hat{B})\cdot\langle\vec{\mathrm{V}}_{11}\rangle/|\hat{F}\times\hat{B}|^2 . \tag{2.51b}$$

Performing the fields expansion, Eq. (2.50), we obtain

$$\mu_c=\frac{\sum_{\vec{k},N}\sum_{\mu,\lambda}\hat{F}\cdot\vec{V}_N(\vec{k})f_N^0(\vec{k})\phi_{N\lambda}^{\delta\mu}(E_N(\vec{k}))K_\lambda^{\delta\mu}(\hat{k})}{\sum_{\vec{k},N}f_N^0(\vec{k})}, \tag{2.52a}$$

$$r\mu_c^2=\frac{\sum_{\vec{k},N}\sum_{\mu,\lambda}(\hat{F}\times\hat{B})\cdot\vec{V}_N(\vec{k})f_N^0(\vec{k})\chi_{N\lambda}^{\delta\mu}(E_N(\vec{k}))K_\lambda^{\delta\mu}(\hat{k})}{|\hat{F}\times\hat{B}|^2\sum_{\vec{k},N}f_N^0(\vec{k})}. \tag{2.52b}$$

It is clear now that due to the vectorial nature of $\vec{V}_N(\vec{k})$ only the δ parts of f_N contribute to the mobilities. Denominators in Eqs. (2.46), (2.52a), and (2.52b) are the total number of carriers in the crystal.

The integrals occurring in Eqs. (2.52a) and (2.52b) can be written in terms of integrals evaluated earlier. The forms we adopt are

$$\mu_c=\frac{1}{\hbar}\hat{F}\cdot\frac{\sum_{N,\mu,\lambda}\int_0^\infty d\mathscr{E}\,e^{-\beta\mathscr{E}}\phi_{N\lambda}^{\delta\mu}(\mathscr{E})\vec{g}_{N\lambda}^{\delta\mu}(\mathscr{E})}{4\pi\sum_N\int_0^\infty d\mathscr{E}\,e^{-\beta\mathscr{E}}\langle\alpha_0|\Gamma_N|\alpha_0\rangle}, \tag{2.53a}$$

where $\beta=(k_BT)^{-1}$, and

$$r\mu_c^2=\frac{\hat{F}\times\hat{B}}{|\hat{F}\times\hat{B}|^2}\cdot\frac{\sum_{N,\mu,\lambda}\int_0^\infty d\mathscr{E}\,e^{-\beta\mathscr{E}}\chi_{N\lambda}^{\delta\mu}(\mathscr{E})\vec{g}_{N\lambda}^{\delta\mu}(\mathscr{E})}{4\pi\sum_N\int_0^\infty d\mathscr{E}\,e^{-\beta\mathscr{E}}\langle\alpha_0|\Gamma_N|\alpha_0\rangle}. \tag{2.53b}$$

Since $\phi^{\delta\mu}\sim\hat{F}\cdot\hat{e}_\mu$ and $\vec{g}^{\delta\mu}\sim\hat{e}_\mu$, Eqs. (2.29) and (2.28), respectively,

$$\mu_c\sim\sum_\mu(\hat{F}\cdot\hat{e}_\mu)(\hat{F}\cdot\hat{e}_\mu)=|\hat{F}|^2=1,$$

so that μ_c is independent of the magnitude and direction of the electric field, as it should be for Ohmic mobility of cubic materials. Similarly, from Eq. (2.43),

$$\chi^{\delta\mu}\sim(\hat{F}\times\hat{B})\cdot\hat{e}_\mu,$$

so that

$$r\mu_c^2=\mu_H\mu_c\sim\sum_\mu\frac{[(\hat{F}\times\hat{B})\cdot\hat{e}_\mu][(\hat{F}\times\hat{B})\cdot\hat{e}_\mu]}{|\hat{F}\times\hat{B}|^2}=1$$

and μ_H is independent of the directions and magnitudes of $\vec{F}$ and $\vec{B}$, as long as they are not parallel.

The symmetry analysis presented in this section, with some modifications, can be carried over to noncubic materials. A main difference will arise due to the fact that the three Cartesian coordinates will no longer be equivalent, and as a result mobilities will be anisotropic.

III. COMPUTATIONAL DETAILS

In order to implement the theory outlined in Sec. II we need to evaluate a number of Brillouin-zone integrals. In all cases the weighting factor is

$$\Gamma_N(\mathscr{E},\hat{k})=\left[\frac{2m_0}{\hbar^2}\right]^{3/2}\gamma_N^{1/2}(\mathscr{E},\hat{k})\frac{d\gamma_N(\mathscr{E},\hat{k})}{d\mathscr{E}}, \tag{3.1}$$

where

$$k_N^2=\left[\frac{2m_0}{\hbar^2}\right]\gamma_N(\mathscr{E},\hat{k})$$

defines $\gamma_N(\mathscr{E},\hat{k})$. The γ_N for all three bands are obtained from the solution of the cubic equation as given by Madarasz, Lang, and Hemenger,[46]

$$H_3\gamma^3+H_2\gamma^2+H_1\gamma+H_0=0, \tag{3.2}$$

where the coefficients H_i are functions of energy and the angle $\hat{k}$. Band parameters A, B, and C for Si are taken to be dimensionless so that γ's come out in rydbergs. One may note that in the parabolic limit

$$E(\vec{k})=\frac{\hbar^2k^2}{2m^*}, \tag{3.3a}$$

$$\gamma(\mathscr{E},\hat{k})=\frac{\hbar^2k^2}{2m_0}=\mathscr{E}\frac{m^*}{m_0}, \tag{3.3b}$$

where m^* is the effective mass for the band and $m_0=\frac{1}{2}$ is the free-electron mass. All of the angular integrals in Sec. II were computed and compared with their isotropic parabolic limit with the use of Eqs. (3.3a) and (3.3b). For small energies the difference between the results for the true bands and the isotropic parabolic limit for Ge was on the order of a few percent.

With all the angular integrals calculated we proceed as follows. Using the expansion coefficients A for the transition rates, we form the S matrix in

Eq. (2.24). The λ',λ'' indices ranged through angular momenta 1, 3, 5, and 5' (for the δ_5' harmonic). The angular momenta for the α_L cubic harmonics were $L=0$, 4, 6, and 8. The S-matrix inversion was performed using the Gauss-Jordan method.[47]

The last sensitive procedure is the evaluation of the energy integrals [(2.53a) and (2.53b)] containing the Boltzmann factor. Here, we use the Gauss-Laguerre integration method with 25 points along the energy scale.[48] All the energy-dependent quantities were evaluated at two separate energy meshes. The "rough" energy mesh had the energy interval of 0.0045 eV and 16 energies from 0.0045 to 0.072 eV. The same quantities were also calculated on a finer mesh near $\mathscr{E}=0$ eV with the mesh size of 0.0135/17 eV; again, 16 energies with that mesh size were used. When necessary, interpolation was done via the Lagrange interpolation[49] using 32 first-principles points along the energy scale.

For comparison with the parabolic limit we derived the expected energy dependences of all the factors in the calculation in that limit. These should also be satisfied by the true bands at sufficiently low-hole energies. At low energies the expansion coefficients A for W_{MN} in Eq. (2.3) are essentially energy independent, as if to a first approximation the bands were parabolic. This makes the scattering matrix proportional to Γ_N^2, so that

$$S\sim\Gamma^2\sim\left[\gamma^{1/2}\frac{d\gamma}{d\mathscr{E}}\right]^2\sim\mathscr{E}\ . \tag{3.4}$$

From (2.17), we also see that $g\sim\mathscr{E}$, so that

$$\phi\sim S^{-1}g\sim\frac{1}{\mathscr{E}}\mathscr{E}\sim\text{const}\ , \tag{3.5}$$

which implies that the numerator in Eq. (2.53a) behaves like $\mathscr{E}$ at low energies.

Next, we observe that, Eq. (2.43),

$$\chi\sim S^{-1}\phi\mathscr{H}\ . \tag{3.6}$$

Equation (2.39) shows that $\mathscr{H}\sim\mathscr{E}^{1/2}$, so that

$$\chi\sim\mathscr{E}^{-1/2} \tag{3.7}$$

and

$$\chi g\sim\mathscr{E}^{1/2}\ . \tag{3.8}$$

Therefore, the numerator in Eq. (2.53b) goes as $\mathscr{E}^{1/2}$. Similarly, we see that the denominators in Eqs. (2.53a) and (2.53b) go as $\mathscr{E}^{1/2}$.

IV. TEST OF THE THEORY AND COMPUTATIONAL PROCEDURE— CALCULATION FOR GERMANIUM

The only two calculations similar in spirit to the present one were performed in the 1960s by Tiersten[1] and Lawaetz[2] for germanium. In order to assure ourselves of the validity of our theory and computational procedure, we performed the calculation for germanium using the same set of input parameters for Ge as did Tiersten and Lawaetz. In practice, this entails a change of about ten lines in our code for silicon.

Table I provides the parameters which serve as an experimental input into this part of the calculation. We have to emphasize that there is a large spread in experimentally measured values of the deformation-potential parameters for Ge. From tabulations of various measured values for a, b, and d for Ge it is apparent that there is a large uncertainty in their magnitudes and, at times, in their signs as well.[2,26,33,50] Since this part of the calculation serves mainly as a check of our computational procedure we adopt Tiersten's set of parameters. This way we assure ourselves of a one-to-one comparison with the earlier works in the field. Moreover, Tiersten and Lawaetz did motivate their selection of the deformation-potential parameters from physical considerations. We then expect that these values are reasonable representations of the experimental state of affairs in measurements for Ge.

With the set of parameters in Table I we have calculated the transition probabilities for Ge in the manner described in our first paper on the subject.[41] These were then fitted to a double cubic harmonic series using the method treated in detail for Si in our second paper.[42] The expansion coefficients A, Eq.

TABLE I. Experimental input parameters used in the mobility calculation for germanium.

Valence-band parameters[a] (dimensionless)		Deformation potentials[a] (eV)		Phonon parameters[a] ρc_s^2 (dyn/cm^2)	
A	−13.27	a	2.0	s=transverse	5.75×10^{11}
B	−8.63	b	−2.1	s=longitudinal	1.53×10^{12}
C	12.4	d	−7.0		

[a]Reference 1; ρ is the mass density and c_s is the phonon speed for branch s.

(2.3), that we calculated for Ge are in closest agreement with those reported by Tiersten for transitions involving the more parabolic H band. In turn, Lawaetz[2] reports that the coefficients he calculated also agree with those of Tiersten.[1]

Before presenting the final mobility results for Ge, we shoud keep in mind a few differences between our respective calculations. We use the three top valence bands by solving the cubic equation, Eq. (3.2), for the valence-band dispersions. As a result, our bands are slightly nonparabolic, whereas Tiersten and Lawaetz use only the two top valence bands which, as a result, are parabolic. We adopt an isotropic phonon spectrum with spherically averaged phonon velocities for the three polarization branches. Tiersten and Lawaetz do use full solutions of the dynamical matrix for the phonon spectra and polarization vectors. Lawaetz shows, however, that the results he obtained are insensitive to this detail.[2]

Upon examination of several intermediate results in our calculation for Ge we have reached several conclusions regarding the validity of the parabolic-limit approximation for this material. We found that in all cases the intermediate quantities such as ϕ, χ, numerators, and denominators of Eqs. (2.53a) and (2.53b) for the H band behaved according to the parabolic limit derived in Eqs. (3.4)—(3.8). On the other hand, the corresponding quantities for the L band of Ge displayed important deviations from that behavior. From Fig. 1 of Kane's paper[38] it can be seen that the H band of Ge is in fact accurately parabolic while the L band is not. The same plots also indicated that our calculation is converged with respect to various angular-momentum sums.

Figures 1 and 2 show the total and partial conductivity and Hall mobilities, respectively, as a function of absolute temperature for Ge. The partial mobilities are defined by the following equation:

$$\mu_{c,H}=\frac{\sum_N p_N \mu_{c,H}^N}{\sum_N p_N}\,, \tag{4.1}$$

where $\mu_{c,H}^N$ are the partial mobilities. Equation (4.1) is motivated by a model where the bands conduct current as a parallel resistor network. In this model, therefore, the band conductivities are additive as though the bands were noninteracting. Since we have shown that the interband scattering is as important as the intraband scattering, the motivation for the model does not hold any longer. Yet, we can still define the partial band mobilities through Eq. (4.1) and draw some conclusions from the results. In the cases of both mobilities the light-hole band mobility is the larger of the two, Figs. 1 and 2, with

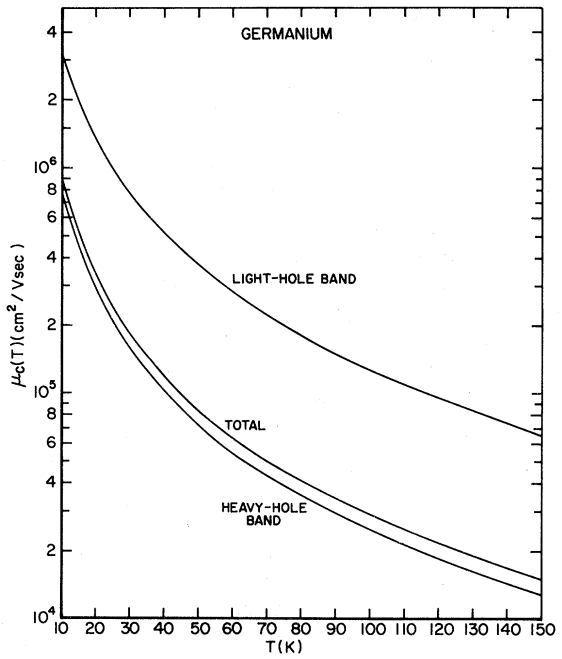

FIG. 1. Calculated total and partial conductivity mobilities, in the acoustic-phonon-limited regime, as a function of temperature.

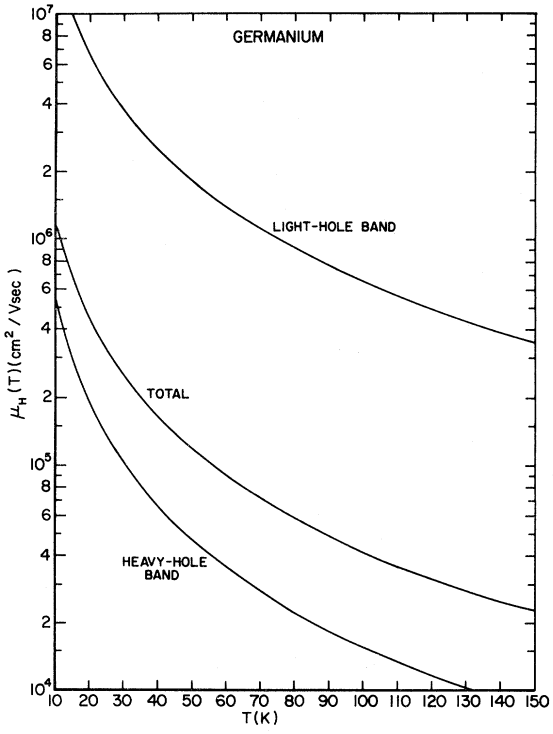

FIG. 2. Calculated total and partial Hall mobilities, in the acoustic-phonon-limited regime, as a function of temperature.

$\mu_c^L/\mu_c^H \sim 5$ and $\mu_H^L/\mu_H^H \sim 40$. Physically, the larger light-hole band mobilities are the consequences of its having a smaller effective mass[19] $M_H/M_L \sim 8$. In the case of the Hall mobility the L band becomes the dominant band in spite of the fact that it contains 20 times fewer holes than the H band. The L band's nonparabolicity, therefore, has its strongest effect on the Hall mobility.

Let us now compare the results of our theoretical formulation of the problem and calculational formalism with the results of calculations by Tiersten and Lawaetz. Tiersten calculated the conductivity mobility for Ge in the parabolic-band approximation using the H and L bands only. With the use of the parameters listed in Table I, Tiersten obtained the expected $T^{-1.5}$ temperature dependence for the conductivity mobility, as did Lawaetz, with

$$\mu_c(100\ \text{K}) = 3.13 \times 10^4$$

in units of $\text{cm}^2/\text{V sec}$. With the use of essentially the same formalism as ours, but with two parabolic bands, Lawaetz states that his 100-K value for μ_c differs from Tiersten's value by about 2%. Our value for the acoustic-phonon-limited conductivity mobility at this temperature is

$$\mu_c(100\ \text{K}) = 2.89 \times 10^4$$

in units of $\text{cm}^2/\text{V sec}$, which differs from Tiersten's result by about 7.7%.

This small difference can be accounted for by several factors which distinguish our respective calculations. One of these might be the precision with which the transition probabilities were fitted to the double cubic harmonic series. We use a far larger sampling of $(\hat{k},\hat{k}')$ scattering directions than Tiersten and a larger number of cubic harmonic pairs for the fit.[42] In addition, we do not treat the L band as parabolic, which is a progressively worse approximation as higher galvanomagnetic coefficients are calculated. On the other hand, Tiersten's more rigorous treatment of the phonon spectrum is an improvement over our isotropic phonon-spectrum approximation. However, we believe that it is the parabolic L-band approximation which accounts for the bulk of the difference.

Figure 3 displays both the calculated r factor for germanium, data to be discussed later, and exponents α_c, α_H in

$$\mu_c = AT^{-\alpha_c}, \tag{4.2}$$

$$\mu_H = BT^{-\alpha_H}. \tag{4.3}$$

The temperature exponent of the conductivity mobility α_c starts out at 10 K with $\alpha_c = 1.498$ and rises monotonically to $\alpha_c = 1.575$ at 120 K. The temperature exponent for the Hall mobility α_H rises steadily from $\alpha_H = 1.420$ at 10 K to $\alpha_H = 1.545$ at 120 K. This represents a rather small temperature variation about the value $\alpha_{c,H} = 1.5$ for strictly parabolic bands.

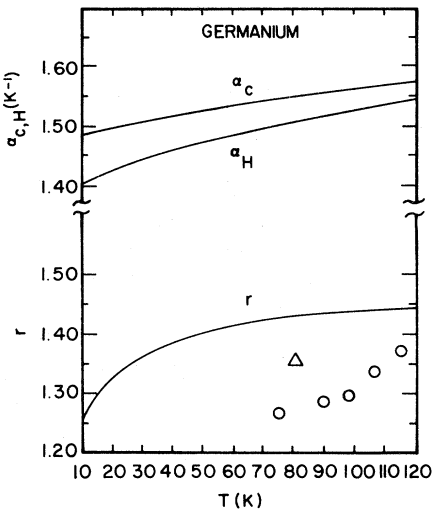

FIG. 3. Top scale: calculated temperature exponents α_c for the conductivity mobility, and α_H for the Hall mobility (solid line). Lower scale: the calculated r factor (solid line) and experimental data of Beer and Willardson (triangles) (Ref. 51, impurity content $1\times10^{13}\ \text{cm}^{-3}$) and Goldberg *et al.* (circles) (Ref. 52, sample D, impurity content $2.4\times10^{13}\ \text{cm}^{-3}$).

It is more difficult to compare our results for μ_H and r with those of Lawaetz (Tiersten did not calculate these quantities). Lawaetz does obtain $\alpha_H = 1.5$, which is the correct exponent for both mobilities in the parabolic-band regime. Our α_H is lower than 1.5 for $T < 70$ K thus reflecting the dominant influence of the light-hole band to μ_H. Lawaetz provides the value of $r = 1.60$ for the choice of the deformation-potential parameters $b = -2$ eV, $d = -7$ eV, and a value of the dilatational deformation potential $a > 0$ which will yield the lowest value for r for acoustic-mode scattering only. The value of $r = 1.60$, therefore, represents the lowest value Lawaetz calculated for acoustic-phonon-limited mobility with fixed b and d, and a positive value for a. From Fig. 3 of Ref. 2 we estimate that for the parameters in Table I Lawaetz obtained $r \sim 1.6$–1.7.

The experimental value for r that Lawaetz used for comparison with the theory is the value of $r = 1.36 \pm 0.07$ at 81 K obtained by Beer and Willardson[51] (sample impurity content $1\times10^{13}\ \text{cm}^{-3}$). This is far below Lawaetz's $r \sim 1.6$–1.7. On the other hand, our result at 81 K is $r = 1.43$, Fig. 3, which is very close to the r of Beer and Willardson,

with the parameters used by Lawaetz.

We can suggest primarily two reasons for the different results of the two theoretical calculations. As we have shown, the light-hole band is quite nonparabolic and dominates the Hall mobility. The L band, therefore, alters μ_H and r from the values calculated in the parabolic approximation. We also have one misgiving about Lawaetz's chosen form for his scattering matrix K (S in our notation). His K matrix, Eq. (3.15) of Ref. 2, uses the completeness relation for cubic harmonics in the second term of K involving the sum over $\mu\nu$. Formally, this is correct, but computationally one has to achieve convergence in the sum over an additional angular-momentum index. The sum over μ can be eliminated by using the completeness relation, and so there will be only one sum over ν to carry to convergence. We feel this would be a safer procedure, considering that in order to calculate μ_H one must use S^{-1} twice, Eqs. (2.29) and (2.43).

Figure 3 also displays the data for sample D of Goldberg *et al.*[52] with the impurity concentration of 2.4×10^{13} cm^{-3} (their sample G was less pure than sample D). Older data of Morin[53] for r is not shown, since the impurity content is unknown, but it generally falls below the data of Goldberg *et al.* Thus by comparison with the data of Goldberg *et al.* the calculated r factor is about 12% too high. It appears that the data of Beer and Willardson coming from a purer sample may be more representative of a high-purity sample with less ionized impurity scattering. By contrast, Nagakawa and Zukotynski[8] calculate $r\sim2.0$ in this temperature range, far above the measured values. Reference 8 also shows that ionized impurity scattering has the effect of dramatically lowering the value of r.

Although it has not been our aim to provide a critical comparison between experiment and theory for Ge, we can offer several suggestions concerning the results. First of all, the data used for comparison in Fig. 3 are in the temperature range where the optical-phonon scattering ought to come in for germanium. Therefore, the data may not be representative of the temperature regime for the acoustic-phonon-limited mobility $T<80$ K. Second, we would have liked to use, for comparison, data obtained from higher-purity samples, on the order of 10^{11} cm^{-3}, for low temperatures, $T<80$ K. No such data for the same sample seems to exist for Ge where both the high and low magnetic field limits were explored to obtain the conductivity and Hall mobilities, respectively. Third, the values of the deformation-potential parameters for Ge are still in doubt. In particular, the compilation of these parameters by Wiley[26] suggests that our value for d is probably too high. We, however, do not feel that the experimental situation here has been resolved enough to warrant another calculation for Ge at this time.

Figure 4 presents the comparison between our calculated conductivity mobility and results of measurements by Ottaviani *et al.*[54] and by Brown and Bray.[55] A rather close agreement is found for $T<80$ K, while for $T>80$ K one can see already the influence of the optical-phonon scattering in the data of Brown and Bray. Also, the 20-K μ_c point of Ottaviani *et al.*[54] may be indicating the presence of ionized impurity scattering. Owing to the lack of the μ_H and μ_c data on the same high-purity sample for low temperatures, we cannot present a comparison with theory for μ_H. For this purpose it is best to consult Fig. 4 for the r factor.

The calculation for germanium has achieved its purpose as a testing ground for the theoretical and computational procedures. We have reproduced the results of earlier μ_c calculations of Tiersten and Lawaetz and improved considerably the results for μ_H by including the nonparabolicity for the L band. The degree of quantitative agreement this calculation has achieved with experiments does indicate that a first-principles approach can be quantitatively successful and confirms the fundamental correctness

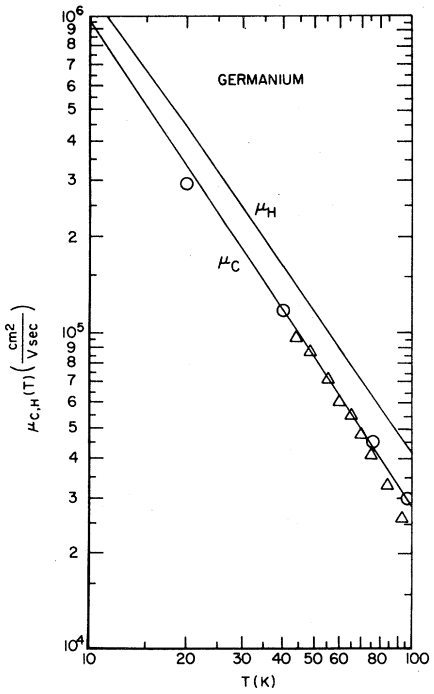

FIG. 4. Calculated conductivity and Hall mobilities (solid lines) and the data for μ_c of Ottaviani *et al.* (circles) (Ref. 54, time-of-flight method, impurity content $<1\times10^{11}$ cm^{-3}) and Brown and Bray (triangles) (Ref. 55, impurity content 1.25×10^{13} cm^{-3}).

TABLE II. Experimental input parameters used in the mobility calculation for silicon.

Valence-band parameters[a] (dimensionless)		Deformation potentials[b] (eV)		Phonon parameters ρc_s^2 (dyn/cm^2)[b]	
A	−4.27	a	2.1	s=transverse	6.804×10^{11}
B	−0.63	b	−2.2	s=longitudinal	18.852×10^{11}
C	4.93	d	−5.3		

[a]Reference 8.
[b]Reference 26; ρ is the mass density and c_s is the phonon speed for branch s.

of the deformation-potential theory. This viewpoint will be reinforced in the next section on Si where a more reliable set of deformation-potential parameters will be used and comparison made with a very recent careful measurement on Si.

V. RESULTS FOR SILICON

The mobility calculation for silicon has been performed using the parameters listed in Table II. The deformation-potential parameters given in Table II are not the ones we used in our two previous publications.[41,42] The two sets of numbers come from two different compilations by Wiley.[26,50] The set used here is the more recent one[26] and, moreover, is in good agreement with the latest piezospectroscopic measurements on Si.[28,36]

Figures 5 and 6 display the calculated partial and total conductivity and Hall mobilities, respectively. As expected, the L band has the more mobile holes and dominates the overall Hall mobility. The spin-orbit band makes a negligible contribution to either calculated mobility. Figure 7 presents the calculated temperature exponents for both mobilities and the r factor for silicon. The α_c coefficient starts out at 10 K with $\alpha_c \sim 1.57$ and after a rapid rise saturates in value at about 2.10 for $T > 90$ K. The rise of α_H from 1.55 to 10 K is monotonic in the temperature range examined. Therefore, it is only at the lowest temperatures that the mobilities come close to the parabolic-band $\mu \sim T^{-1.5}$ behavior. Also shown in Fig. 7 are temperature exponents $\alpha_c \sim 1.75 \pm 0.05$

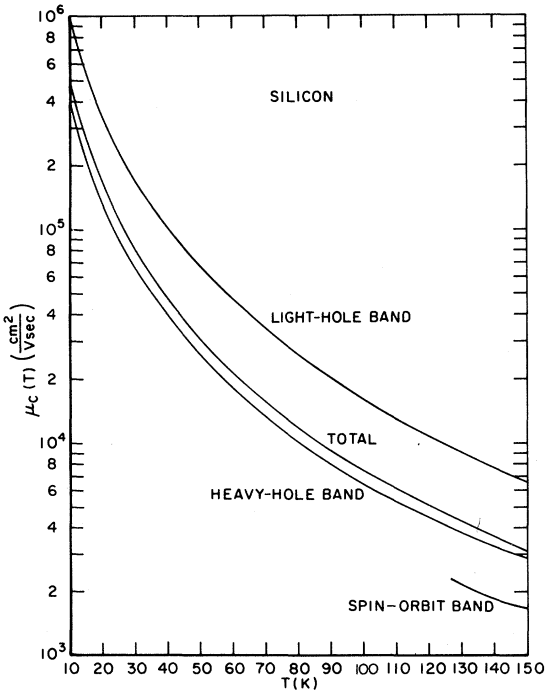

FIG. 5. Same as Fig. 1 for silicon.

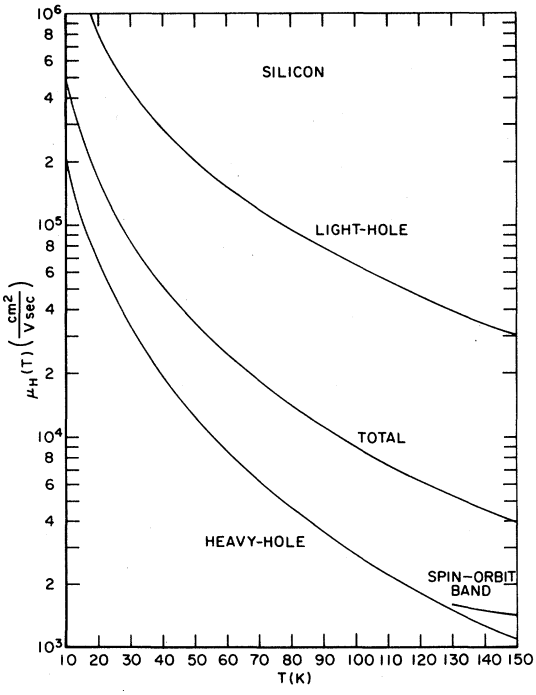

FIG. 6. Same as Fig. 2 for silicon.

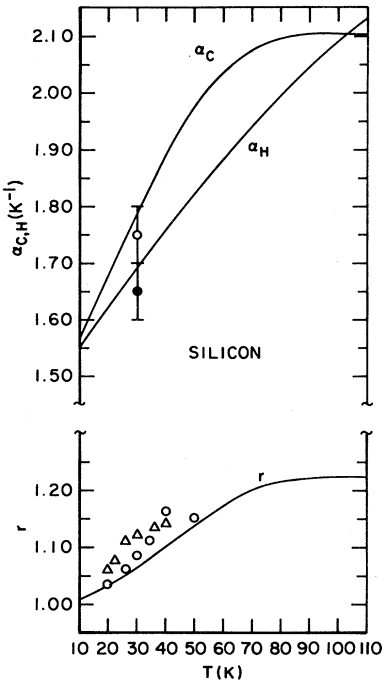

FIG. 7. Same as Fig. 3 for silicon. Experimental data for α_c (open circle) and α_H (solid circle) from Mitchel and Hemenger.[56] The r-factor data of Mitchel and Hemenger is from sample 1202-H (triangles) (Hall bar, acceptors, 6.57×10^{11} cm^{-3}, donors 3.96×10^{11} cm^{-3}) and sample 1300-V (circles) (Van der Pauw configuration, acceptors 9.14×10^{11} cm^{-3}, donors 3.33×10^{11} cm^{-3}).

and $\alpha_H \sim 1.65\pm0.05$ measured by Mitchel and Hemenger[56] in the (20—40)-K range on a high-purity silicon sample.

Figure 7 shows a generally close agreement between experiment and theory for the exponents. Since only one exponent was fitted to the experimental data it is difficult to say whether the exponents have an appreciable temperature dependence themselves. Measurements encounter difficulties at lower temperatures, $T<20$ K, due to the lack of signal connected with a low thermal hole population in high-purity samples. Using lower-purity samples complicates matters due to the presence of ionized impurity scattering. At higher temperatures, $T>40$ K, the problem is the attainability of high enough magnetic fields to saturate the Hall coefficient. One must remember that this saturation is more difficult to achieve for heavy holes due to their lower mobility. On the other hand, the large light-hole mobilities impose more stringent requirements on the electric fields in order to stay within the Ohmic regime.

The calculated and measured r factors are also displayed in Fig. 4. The two sets of data from Mitchel *et al.*[56] correspond to sample 1202-H (Hall bar configuration, $N_A=6.57\times10^{11}$ cm^{-3}, $N_D=3.96\times10^{11}$ cm^{-3}) and sample 1300-V (Van der Pauw configuration, $N_A=9.14\times10^{11}$ cm^{-3}, $N_D=3.33\times10^{11}$ cm^{-3}). The difference between the two sets of experimental data probably reflects the degree of electric field uniformity for both sample geometries. The r factor is lower for sample 1300-V for possibly this reason and also possibly due to its higher impurity content. Considering the spread of experimental data the agreement between experiment and theory is very good and is on the order of 4%.

Figure 8 shows the comparison between the calculated conductivity mobility and the high-field limit of the Hall mobility measured by Mitchel *et al.*[56] (sample 1202-H). The agreement is seen to be very good. There is a hint at lower temperatures of the influence of ionized impurity scattering in the data since the first two points fall slightly below the calculated curve. If this conjecture were to be true it would change the exponent α_c in Fig. 8 and make it more positive, in better agreement with the calculated α_c.

The low-field limit of the Hall mobility, as measured by Mitchel *et al.*,[56] and other data of Elstner,[57] together with the calculated Hall mobility,

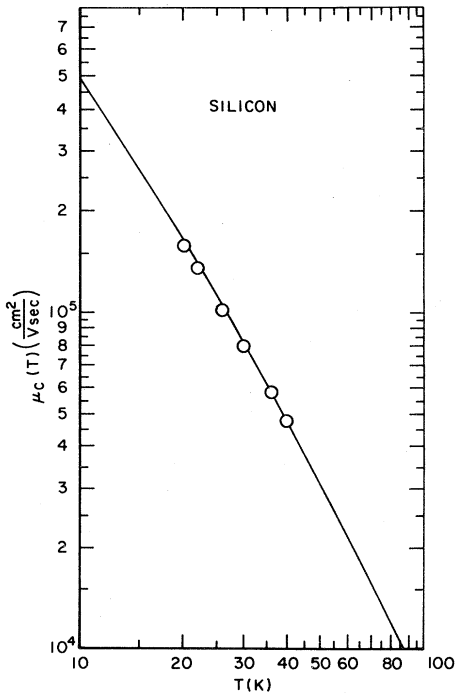

FIG. 8. Calculated conductivity mobility for silicon (solid line) and the experimental data of Mitchel and Hemenger (Ref. 56) for sample 1202-H.

are shown in Fig. 9. Again, the agreement found here is very good. It is expected that at about 100 K the influence of the optical-phonon scattering will be felt. The theory presented in this paper can be extended to include that scattering mechanism as well, as was done for Ge by Lawaetz.[2] Note that these two phonon scattering mechanisms are in competition with one another. Therefore, our S matrix, Eq. (2.24), will consist of two parts,

$$S = S_{\text{ac}} + S_{\text{opt}} , \tag{5.1}$$

for the acoustic and optical phonons. Clearly, to solve for the mobilities we need to invert S, e.g., Eqs. (2.29) and (2.43),

$$S^{-1} = (S_{\text{ac}} + S_{\text{opt}})^{-1} , \tag{5.2}$$

which is not the same as

$$S^{-1} = S_{\text{ac}}^{-1} + S_{\text{opt}}^{-1} . \tag{5.3}$$

This last generally unacceptable approximation leads to the often used expression

$$\mu^{-1} = \sum_i \mu_i^{-1} , \tag{5.4}$$

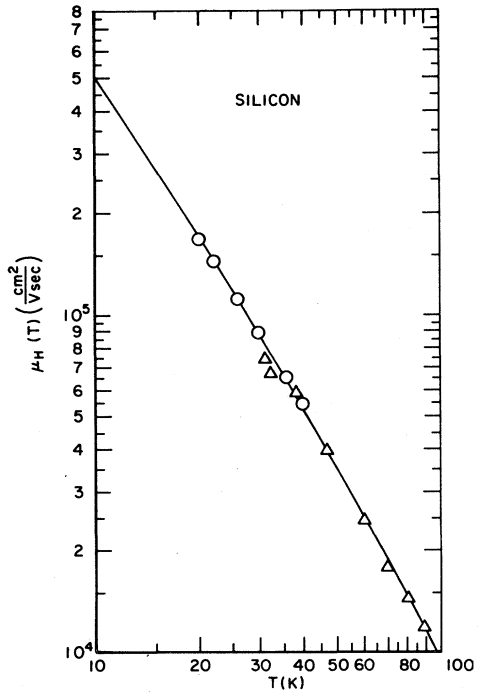

FIG. 9. Calculated Hall mobility for silicon (solid line) and the experimental data of Mitchel and Hemenger (Ref. 56) for sample 1202-H (circles), and the data of Elstner (Ref. 57) (triangles) (acceptors 1.0×10^{13} cm^{-3}, donors 6.5×10^{10} cm^{-3}).

where the inverse of mobilities for each scattering mechanism is added. We shall summarize results of this calculation in the next section.

VI. SUMMARY AND CONCLUSIONS

The conductivity and Hall mobilities for silicon and germanium have been calculated using the deformation-potential theory of Tiersten[1] and the formalism developed by Lawaetz.[2] We have solved the Boltzmann equation without recourse to the relaxation-time approximation. The agreement between experimental and theoretical r factors is on the order of 4% for silicon and 12% for germanium. The corresponding mobilities are generally in better agreement with the experiments than are the r factors.

The results of our calculation of the conductivity and Hall mobilities for Si and Ge, together with the pioneering works of Tiersten and Lawaetz, indicate that phonon-limited transport in nonpolar semiconductors can be quantitatively modeled within the framework of the first-principles deformation-potential theory. It appears that the main limitation to the quantitative accuracy of the method is the precision with which the deformation potentials are known, other input parameters having already been determined with sufficient precision.

Elimination of a few approximations in our theoretical treatment can make the theoretical results more exact but that might be beyond the resolution of present-day experiments. These approximations, taken together with the inherent limitations of the deformation-potential concept itself, can be estimated to produce a $\pm10\%$ fundamental accuracy of the method employed here.[1,2] These approximations will produce worse agreement for progressively higher transport coefficients, e.g., longitudinal and transverse magnetoresistance, etc.

The lowest-temperature results would be improved by retaining the phonon energy in the δ-function argument, Eq. (2.3). Another improvement would result from the use of the dynamical matrix solutions for phonon energies and polarization vectors. By using a degenerate perturbation theory, one also ought to eliminate the ambiguity in defining the polarization vectors in the $\vec{q}\to0$ limit for forward intraband hole scattering.[1,2] Finally, as Lawaetz has shown,[58] the deformation-potential scattering theory is only the first-order long-wavelength approximation to the full carrier-phonon interaction term. This approximation, he shows, is good to at least 5%, which provides the limit on the accuracy of the method itself.

ACKNOWLEDGMENTS

This work was performed under U.S. Air Force Contract Nos. F33615-78-C-5064 and F33615-81-C-5095 at the Materials Laboratory, Wright-Patterson U.S. Air Force Base, Ohio. We are indebted to Dr. P. M. Hemenger of the Materials Laboratory and Mr. John A. Detrio of the University of Dayton Research Institute for their long-standing support of this work. We would also like to acknowledge Dr. R. S. Allgaier, Dr. P. J. Price, Dr. M. Tiersten, Dr. J. C. Hensel, Dr. S. Zukotynski, Dr. C. Elbaum, Dr. J. E. Lang, and Dr. W. Mitchell for many helpful discussions.

[1]M. Tiersten, IBM J. Res. Dev. 5, 122 (1961); J. Phys. Chem. Solids 25, 1151 (1964).
[2]P. Lawaetz, Phys. Rev. 174, 867 (1968).
[3]G. L. Bir and G. E. Pikus, Fiz. Tverd. Tela (Leningrad) 1, 1642 (1959) [Sov. Phys.—Solid State 1, 1502 (1960)]; 2, 2287 (1960) [2, 2039 (1960)].
[4]G. L. Bir, E. Normantas, and G. E. Pikus, Fiz. Tverd. Tela (Leningrad) 4, 1180 (1962) [Sov. Phys.—Solid State 4, 867 (1962)].
[5]C. Herring and E. Vogt, Phys. Rev. 101, 944 (1956).
[6]W. P. Dumke, Phys. Rev. 101, 531 (1956); Phys. Rev. B 2, 987 (1970).
[7]P. P. Debye and E. M. Conwell, Phys. Rev. 93, 693 (1954).
[8]H. Nakagawa and S. Zukotynski, Can. J. Phys. 55, 1485 (1977); 56, 364 (1977).
[9]S. S. Li, Solid-State Electron. 21, 1109 (1978).
[10]L. C. Linares and S. S. Li, J. Electrochem. Soc. 128, 601 (1981).
[11]J. F. Liu, S. S. Li, L. C. Linares, and K. W. Teng, Solid-State Electron. 24, 827 (1981).
[12]M. Costato, S. Fontanesi, and L. Reggiani, J. Phys. Chem. Solids 34, 547 (1973).
[13]M. Costato, and L. Reggiani, Phys. Status Solidi B 58, 471 (1973).
[14]G. Ottaviani, L. Reggiani, C. Canali, F. Nava, and A. Alberigi-Quaranta, Phys. Rev. B 12, 3318 (1975).
[15]L. Reggiani, C. Canali, F. Nava, and G. Ottaviani, Phys. Rev. B 16, 2781 (1977).
[16]G. Gagliani and L. Reggiani, Nuovo Cimento B 30, 207 (1975).
[17]C. Canali, C. Jacoboni, F. Nava, G. Ottaviani, and A. Alberigi-Quaranta, Phys. Rev. B 12, 2265 (1975).
[18]S. Bosi, C. Jacoboni, and L. Reggiani, J. Phys. C 12, 1525 (1979).
[19]M. Costato, G. Gagliani, C. Jacoboni, and L. Reggiani, J. Phys. Chem. Solids 35, 1605 (1974).
[20]M. Asche and J. von Borzeszkowski, Phys. Status Solidi 37, 433 (1970).
[21]J. von Borzeszkowski, Phys. Status Solidi B 73, 607 (1976).
[22]A. Hackmann, D. Neubert, V. Scherz, and R. Schlief, Phys. Rev. B 24, 4666 (1981).
[23]K. Takeda, K. Sakui, and M. Sakata, J. Phys. C 15, 767 (1982).
[24]D. L. Rode, Phys. Rev. B 2, 1012 (1970); Phys. Status Solidi B 55, 687 (1973); in *Semiconductors and Semimetals,* edited by R. K. Willardson and Albert Beer (Academic, New York, 1975), Vol. X, pp. 1—89.
[25]J. D. Wiley and M. D. Domenico, Jr., Phys. Rev. B 2, 427 (1970).
[26]J. D. Wiley, Phys. Rev. B 4, 2485 (1971); in *Semiconductors and Semimetals,* edited by R. K. Willardson and Albert Beer (Academic, New York, 1975), Vol. X, pp. 91—171.
[27]L. J. Challis and S. C. Haseler, J. Phys. C 11, 4681 (1978).
[28]J. C. Merle, M. Capizzi, and P. Fiorini, Phys. Rev. B 17, 4821 (1978), see Table III.
[29]K. Suzuki and J. C. Hensel, Phys. Rev. B 9, 4184 (1974).
[30]J. C. Hensel and K. Suzuki, Phys. Rev. B 9, 4219 (1974).
[31]T. Fjeldly, T. Ishiguro, and C. Elbaum, Phys. Rev. B 7, 1392 (1973).
[32]K. Hess, J. Phys. Chem. Solids 33, 139 (1971).
[33]M. Costato and L. Reggiani, Lett. Nuovo Cimento IV, 848 (1970).
[34]I. Balslev, Phys. Rev. 143, 636 (1966).
[35]R. H. Parmenter, Phys. Rev. 99, 1767 (1955).
[36]H. R. Chandrasekhar, P. Fischer, A. K. Ramdas, and S. Rodriguez, Phys. Rev. B 8, 3836 (1973), see Table V.
[37]E. B. Hale and T. G. Castner, Jr., Phys. Rev. B 1, 4763 (1970).
[38]Evan O. Kane, J. Phys. Chem. Solids 1, 249 (1957).
[39]G. D. Whitfield, Phys. Rev. 121, 720 (1961).
[40]P. J. Price, IBM J. Res. Dev. 1, 147 (1957); 1, 239 (1957); 2, 200 (1958).
[41]F. L. Madarasz and F. Szmulowicz, Phys. Rev. B 24, 4611 (1981).
[42]Frank Szmulowicz and Frank L. Madarasz, Phys. Rev. B 26, 2101 (1982).
[43]J. F. Cornwell, *Group Theory and Electronic Energy Bands in Solids* (Wiley, New York, 1969), pp. 35, 60, and 61.
[44]F. C. Von der Lage and H. Bethe, Phys. Rev. 71, 612 (1947).
[45]F. Seitz, Phys. Rev. 79, 372 (1950).
[46]F. L. Madarasz, J. E. Lang, and P. Hemenger, J. Appl. Phys. 52, 4646 (1981). Equation (10a) of this reference should read $\eta=\sqrt{2}\sin\phi$.
[47]Daniel D. McCracken, *Fortran with Engineering Applications* (Wiley, New York, 1967), p. 161.
[48]A. H. Stroud and Don Secrest, *Gaussian Quadrature*

Formulas (Prentice-Hall, Englewood Cliffs, 1966), p. 253.

[49]Philip J. Davis and Ivan Polonsky, in *Handbook of Mathematical Functions with Formulas, Graphs, and Mathematical Tables,* edited by Milton Abramowitz and Irene A. Stegun (U.S. GPO, Washington, D.C., 1972), p. 878.

[50]J. D. Wiley, Solid State Commun. 8, 1865 (1970).

[51]A. C. Beer and R. K. Willardson, Phys. Rev. 100, 1286 (1958).

[52]C. Goldberg, E. N. Adams, and R. E. Davis, Phys. Rev. 105, 865 (1957).

[53]F. J. Morin, Phys. Rev. 93, 62 (1954).

[54]G. Ottaviani, C. Canali, F. Nava, and J. W. Mayer, J. Appl. Phys. 42, 2917 (1973).

[55]D. M. Brown and R. Bray, Phys. Rev. 127, 1593 (1962).

[56]W. C. Mitchel and P. M. Hemenger, J. Appl. Phys. 53, 6880 (1982).

[57]L. Elstner, Phys. Status Solidi 17, 139 (1966).

[58]P. Lawaetz, Phys. Rev. 183, 730 (1969).